

Real-time measurement of Brownian relaxation of magnetic nanoparticles by a mixing-frequency method

Liang Tu, Ying Jing, Yuanpeng Li, and Jian-Ping Wang

Citation: *Appl. Phys. Lett.* **98**, 213702 (2011);

View online: <https://doi.org/10.1063/1.3595273>

View Table of Contents: <http://aip.scitation.org/toc/apl/98/21>

Published by the [American Institute of Physics](#)

Articles you may be interested in

[Biological sensors based on Brownian relaxation of magnetic nanoparticles](#)

Applied Physics Letters **85**, 2971 (2004); 10.1063/1.1801687

[Magnetic-field dependence of Brownian and Néel relaxation times](#)

Journal of Applied Physics **119**, 043903 (2016); 10.1063/1.4940724

[Biological sensing with magnetic nanoparticles using Brownian relaxation \(invited\)](#)

Journal of Applied Physics **97**, 10R101 (2005); 10.1063/1.1853694

[A simulation study on superparamagnetic nanoparticle based multi-tracer tracking](#)

Applied Physics Letters **107**, 173701 (2015); 10.1063/1.4934743

[Superparamagnetic nanoparticle-based viscosity test](#)

Applied Physics Letters **107**, 053701 (2015); 10.1063/1.4928057

[Measurement of molecular binding using the Brownian motion of magnetic nanoparticle probes](#)

Applied Physics Letters **96**, 033702 (2010); 10.1063/1.3291063

Scilight

Sharp, quick summaries **illuminating**
the latest physics research

Sign up for **FREE!**

AIP
Publishing

Real-time measurement of Brownian relaxation of magnetic nanoparticles by a mixing-frequency method

Liang Tu, Ying Jing, Yuanpeng Li, and Jian-Ping Wang^{a)}

Department of Electrical and Computer Engineering, University of Minnesota, Minneapolis, Minnesota 55455, USA

(Received 5 April 2011; accepted 5 May 2011; published online 26 May 2011)

A detection scheme for real-time Brownian relaxation of magnetic nanoparticles (MNPs) is demonstrated by a mixing-frequency method in this paper. MNPs are driven into the saturation region by a low frequency sinusoidal magnetic field. A high frequency sinusoidal magnetic field is then applied to generate mixing-frequency signals that are highly specific to the magnetization of MNPs. These highly sensitive mixing-frequency signals from MNPs are picked up by a pair of balanced built-in detection coils. The phase delays of the mixing-frequency signals behind the applied field are derived, and are experimentally verified. Commercial iron oxide MNPs with the core diameter of 35 nm are used for the measurement of Brownian relaxation. The results are fitted well with Debye model. Then a real-time measurement of the binding process between protein G and its antibody is demonstrated using MNPs as labels. This study provides a volume-based magnetic sensing scheme for the detection of binding kinetics and interaction affinities between biomolecules in real time. © 2011 American Institute of Physics. [doi:10.1063/1.3595273]

Magnetic nanoparticle (MNP) detection for biological and medicinal applications has been achieved by a variety of sensing schemes. The search-coil based sensing scheme is one of the good candidates among them for future point-of-care devices and systems because of its following unique integrated features: relatively high sensitivity at room temperature,¹ dynamic volume detection (nonsurface binding), intrinsic superiority to measure ac magnetic field, functionality as an antenna for wireless information transmission, and application driven properties such as low cost, portability, and easy to use. In traditional ac magnetic susceptibility measurement such as Physical Property Measurement System,² DynoMag Susceptometer,³ and Slit Toroid Device,⁴ a pair of balanced coils picks up the magnetization of the sample under an ac magnetic field and a lock-in amplifier or impedance analyzer is used to detect the complex ac susceptibility. However, this method suffers from high background fluctuation due to the thermal and mechanical instability of the coils, as well as the magnetic moment contribution from sample matrix (e.g., water) and/or container (e.g., plastic tube). Given the small amount of MNPs sample in the paramagnetic or diamagnetic environment, the background is a significant portion of the overall signal. In contrast, a mixing-frequency method⁵ has been used to detect the nonlinear magnetization of MNPs per testing sample by measuring the amplitude of the mixing frequency signals and thereby avoid the high noise at the fundamental frequencies.^{6,7} A magnetic field with low frequency (e.g., $f_2=10$ Hz) and large amplitude drives the MNPs into their nonlinear saturation region periodically. Another magnetic field with higher frequency (e.g., $f_1=20$ kHz), and with a relatively small amplitude due to the inductance of excitation coil, is used to transfer the nonlinearity into the mixing frequency signals, such as f_1+2f_2 (20.02 kHz). In this higher frequency region, the detection coil has higher output voltage

amplitude, and the measurement system has lower $1/f$ noise, thus the mixing-frequency method can greatly improve the signal-to-noise ratio.

In this letter, we propose and demonstrate a search coil based susceptometry to measure the real-time Brownian relaxation of MNPs by the mixing-frequency method. In previous studies,^{8,9} the changes in Brownian relaxation before and after the binding events were experimentally shown by searching the peak of imaginary susceptibility in the entire frequency domain. This method faces a challenge for a real-time measurement. We address this challenge in this letter. Phase delay of the mixing-frequency signal is measured along the frequency of one of applied sweeping ac fields. We show that the phase delay is highly related to the relaxation time of MNPs, which enables monitoring the Brownian relaxation process of MNPs in real time.

Superparamagnetic nanoparticles with small sizes are typically being used for biological applications to avoid the aggregation as well as any negative influence without external field. Its magnetization curve can be expressed as follows:

$$M = M_S \times L\left(\frac{m_0\mu_0 H}{k_B T}\right), \quad (1)$$

where M_S is the saturation magnetization, m_0 is the magnetic moment of a single particle, μ_0 is the magnetic permeability of vacuum, H is the applied field, k_B is the Boltzmann constant, T is the absolute temperature, and L is the Langevin function.

Two sinusoidal magnetic fields are applied simultaneously as follows: one with low amplitude A_1 , high frequency f_1 , written as $A_1 \cos(2\pi f_1 t)$; the other with high amplitude A_2 , low frequency f_2 , written as $A_2 \cos(2\pi f_2 t)$. The sum of these two fields (H) is transferred to magnetization (M) by Langevin function. Taylor Expansion near zero magnetization shows that, besides the linear response, the major mixing components are as the following:⁶

^{a)}Author to whom correspondence should be addressed. Electronic mail: jpwang@umn.edu.

$$[A_1 \cos(2\pi f_1 t) + A_2 \cos(2\pi f_2 t)]^3 = \dots + \frac{3}{4} A_1 A_2^2 \cos[2\pi(f_1 \pm 2f_2)t] + \dots \quad (2)$$

There are two relaxation mechanisms for MNPs. The physical rotation of particle in the viscous medium is called Brownian relaxation, and magnetic dipole flipping inside a stationary particle is called Néel relaxation. Brownian relaxation depends on an effective hydrodynamic volume. Néel relaxation depends on magnetic volume. The total relaxation process is a parallel model of these two relaxation schemes, but Brownian relaxation dominates when MNP's diameter is large, e.g., iron oxide MNP's diameter is larger than 20 nm;¹⁰

$$\tau_{\text{total}} \approx \tau_B = \frac{3\eta V_H}{k_B T}, \quad (3)$$

where η is the viscosity of the carrier or matrix fluid and V_H is the effective hydrodynamic volume of MNP.

When the frequency of ac applied field is low, the particles' magnetization can follow the excitation field tightly, and the susceptibility χ is a real number. As the excitation frequency increases, the particles' magnetization cannot follow the excitation field, and the relaxation processes introduce a phase in the complex ac susceptibility. The relationship between relaxation time τ and phase φ of ac susceptibility can be calculated using Debye model.¹¹

$$\chi(\omega) = \frac{\chi_0}{1 + j\omega\tau} = \frac{\chi_0}{\sqrt{1 + (\omega\tau)^2}} e^{-j \tan^{-1}(\omega\tau)} = |\chi| e^{j\varphi}, \quad (4)$$

where χ_0 is the static susceptibility and ω is the angular frequency. Assuming the particles' magnetization has a phase delay φ_1 to the high frequency field and a phase delay φ_2 to the low frequency field, the mixing-frequency component of magnetization becomes as follows:

$$[A_1 \cos(2\pi f_1 t - \varphi_1) + A_2 \cos(2\pi f_2 t - \varphi_2)]^3 = \dots + \frac{3}{4} A_1 A_2^2 \cos[2\pi(f_1 + 2f_2)t - \varphi_1 - 2\varphi_2] + \dots \quad (5)$$

The total relaxation phase $\varphi_1 + 2\varphi_2$ can therefore be determined by measuring the phase of the mixing frequency at $f_1 + 2f_2$. If one frequency (e.g., f_2) is fixed, and the other frequency (e.g., f_1) is swept, the relaxation phase $\varphi_1 + 2\varphi_2$ along f_1 will show the relationship between φ_1 and f_1 . Either one of f_1 and f_2 can be swept depending on whether high frequency region or low frequency region is of interest.

Our search-coil based Susceptometry setup includes two excitation coils that generate 10 Hz ac field with 100 Oe amplitude and 20 kHz ac field with 10 Oe amplitude, respectively. One pair of pick up coils with differentially wounded 500 rounds is installed. An instrumentation amplifier connected to a digital acquisition card (DAQ) is used for the signal amplification. LABVIEW program for the instrument control and MATLAB program for signal processing are installed in the computer for controlling the whole setup. Three commercial iron oxide MNPs samples (Ocean NanoTech, Springdale, AR) are used for Brownian relaxation study: SHP35 (MNPs with 35 nm core size, 4 nm oleic acid, and amphiphilic polymer coating, 0.1 ml, 5 mg/ml in H₂O-carboxylic acid solution), IPG35 (SHP35 conjugated with around 10 nm protein G layer, 0.1 ml, 1 mg/ml), and IPG35-Ab (IPG35 conjugated with around 10 nm Goat anti-Human IgG (an antibody isotype of mammals) HRP with ratio 1:100, 0.1 ml, 1 mg/ml). Particle size distributions are

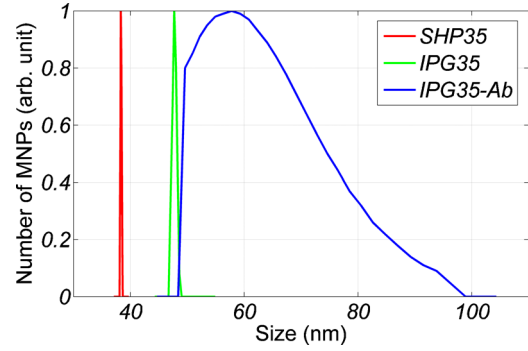


FIG. 1. (Color online) Size distributions of SHP35 (left), IPG35 (middle) and IPG35-Ab (right) samples measured by DLS.

measured by a dynamic light scattering (DLS) instrument ("90 Plus Particle Sizer," Brookhaven Instruments Corp., Holtsville, NY) and are shown in the Fig. 1. The DLS measurement results are consistent with the data provided by Ocean NanoTech. All the three samples are from the same batch of 35 nm iron oxide MNP core, so the wide hydrodynamic size distribution of IPG35-Ab shows that IPG35 binds with antibodies in a range of binding affinity. This is also confirmed by an independent gel electrophoresis measurement (results not shown here).

We measured the MNPs' phase delay of these three samples under ac fields. Phase delay of the mixing-frequency signal is measured by scanning the frequency of f_1 up to 10 kHz. The results of 10 times average are shown in Fig. 2. To prevent any temperature drift due to joule heating of the coil, tone bursts are applied rather than continuous ac field. The experimental results are fitted by the Debye model in Eq. (4). Since the particles are not monodispersed, the total susceptibility comes from the contributions of all MNPs with various sizes. As shown in the Fig. 2, Debye model with the superposition of MNPs' hydrodynamic size distribution¹² is a good fit in our case, although it is argued that Debye model is only valid for small-amplitude (<1 kA/m) (Ref. 13) low-frequency¹⁴ applied ac field and a high frequency susceptibility χ_∞ is needed for the Debye fitting.

The binding process of the antibody to protein coated MNPs solution is detected by monitoring real time relaxation. Instead of the time-consuming whole frequency scan, the frequency f_1 is fixed at a 4 kHz due to the high signal-to-noise ratio around this frequency region (detection coil is

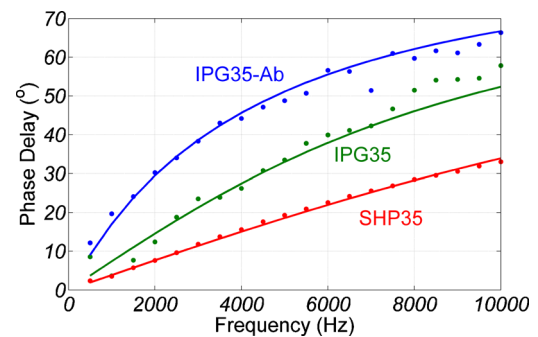


FIG. 2. (Color online) Experimental plots (dots) of phase delay of mixing-frequency $f_1 + 2f_2$ along scanning frequency f_1 for three MNP samples in water solution. Debye model (solid lines) with the superposition of MNPs size distribution shown in Fig. 2 is plotted to compare with the experimental data.

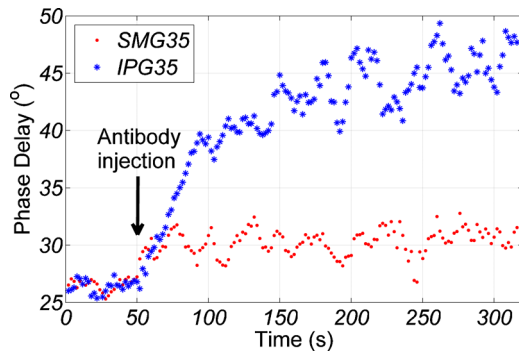


FIG. 3. (Color online) Real time measurement of phase delay of IPG35 in blue (upper curve) and control sample SMG35 in red (lower curve), with antibody injection at the 50th second.

not sensitive in lower frequency region while MNP has low ac susceptibility in higher frequency region). 0.05 ml antibody (goat antihuman IgG HRP conjugated, 5 mg/ml) is dropped onto 0.1 ml IPG35 sample. The antibody sample will then diffuse slowly into IPG35 solution, and gradually bind to protein G on the surface of MNPs, until protein G binding sites on MNPs are saturated with antibody and has the same hydrodynamic size distribution as the standard IPG35-Ab sample prepared by the Ocean NanoTech. On the surface of IPG35 MNPs where protein G is not attached, hydrophilic polyethyleneglycol (PEG) is coated to block nonspecific binding. Both the phase transition (Fig. 3) and amplitude transition (not shown here) during protein G—antibody binding process are recorded. After the antibody is added to the sample at the 50th second, the detected amplitude of the mixing frequency is dropping sharply because the sample gets diluted (away from the center of the detection coil), and also binding events will decrease the MNPs' susceptibility $|\chi|$ as shown in Eq. (4). The amplitude of susceptibility has been used to determine particle clustering and binding¹⁵ but it is heavily affected by the spatial distribution and concentration of the MNPs. In contrast, the phase information records the binding process reliably. As shown in Fig. 3, the antibody solution is added into IPG35 solution at 50th second. As antibodies diffuse into IPG35 solution and bind with MNPs, the phase delay of magnetization then begins to increase, and gradually reaches a plateau which is very close to that of the standard IPG35-Ab. The control experiment is conducted by dropping 0.05 ml antibodies into 0.1 ml SMG35 (SHP35 conjugated with around 10 nm PEG layer, 1 mg/ml). The phase delay measurement shows very little increase because PEG out layer of SMG35 MNPs effectively blocks the nonspecific binding between MNPs and antibodies. The slight increase is possibly because of the higher viscosity from the abundant antibodies in the solution. The experimental and control results show that our system accurately detects the binding between the protein G and antibodies in real time. There are two sources for the relatively large noise for the real time phase delay measurement. Since the MNPs concentration decreases due to dilution, the output signal amplitude decreases and the phase delay measurement suffers from smaller signal-to-noise ratio. Another noise source is from the digitization device when measuring the small mixing frequency signals buried in the large carrier frequency signals. Dynamic carrier tone

cancellation scheme¹⁶ can be implemented to reduce the noise and this is in progress.

Another method to determine the binding process is to use the ratio of higher harmonics from the nonlinear magnetization.¹⁷ The main idea is that when hydrodynamic size increases, the MNPs relax slower and are less likely to reach saturation region, thus the nonlinearity of magnetization changes. In our case, the ratio between amplitude at $f_1 + 2f_2$ and at $f_1 + 4f_2$ is tracked along with phase measurement during the binding process. The results of amplitude ratio are much less sensitive than the phase measurement, and the results are much harder to be interpreted into binding properties. However, the amplitude ratio of higher harmonics contains rich information of nonlinear magnetization and may complement phase measurement to study the MNPs.

In summary, we have developed a technique to detect the real-time relaxation of MNPs by using the mixing-frequency method. Correlation between the phase of the mixing frequency term and the Brownian relaxation of the MNPs was theoretically derived. Experimentally three MNPs (SHP35, IPG35, and IPG35-Ab) have been measured, and the results were fitted by Debye model with the consideration of MNPs size distribution. Real-time measurement of binding process between MNP-labeled protein G and antibody was demonstrated along with a control experiment. This study shows the potential capability of the developed technique for fundamental biological research, disease diagnostic and drug discovery.

Authors thank the partial support from National Science Foundation Grant No. BME 0730825 and Institute of Engineering in Medicine at University of Minnesota. Parts of this work were carried out using the Characterization Facility which receives partial support from NSF through the NSF Minnesota MRSEC Program under Award No. DMR-0819885 and NNIN program.

¹J. Lenz, *Proc. IEEE* **78**, 973 (1990).

²Q. Design, San Diego, CA, <http://www.qdusa.com/products/ppms.html>.

³Imago Institute, Göteborg, SWEDEN, <http://www.imago.com/Products/dynomag/index.aspx>.

⁴P. C. Fannin and B. K. P. Scaife, *J. Magn. Magn. Mater.* **72**, 95 (1988).

⁵T. L. Paoli and J. F. Svacek, *Rev. Sci. Instrum.* **47**, 1016 (1976).

⁶P. I. Nikitin, P. M. Vetoshko, and T. I. Ksenevich, *J. Magn. Magn. Mater.* **311**, 445 (2007).

⁷H.-J. Krause, N. Wolters, Y. Zhang, A. Offenhausser, P. Miethe, M. H. F. Meyer, M. Hartmann, and M. Keusgen, *J. Magn. Magn. Mater.* **311**, 436 (2007).

⁸S. H. Chung, A. Hoffmann, S. D. Bader, C. Liu, B. Kay, L. Makowski, and L. Chen, *Appl. Phys. Lett.* **85**, 2971 (2004).

⁹Y. Bao, A.B. Pakhomov, and K. M. Krishnan, *J. Appl. Phys.* **99**, 08H107 (2006).

¹⁰R. E. Rosensweig, *J. Magn. Magn. Mater.* **252**, 370 (2002).

¹¹M. I. Shliomis and Yu. L. Raikher, *IEEE Trans. Magn.* **16**, 237 (1980).

¹²K. Enpuku, T. Tanaka, Y. Tamai, F. Dang, N. Enomoto, J. Hojo, H. Kan-zaki, and N. Usuki, *Jpn. J. Appl. Phys.* **47**, 7859 (2008).

¹³C. Mac Oireachtaigh and P. C. Fannin, *J. Magn. Magn. Mater.* **320**, 871 (2008).

¹⁴B. K. P. Scaife, *J. Phys. D: Appl. Phys.* **19**, L195 (1986).

¹⁵C. Hong, C. C. Wu, Y. C. Chiu, S. Y. Yang, H. E. Hornig, and H. C. Yang, *Appl. Phys. Lett.* **88**, 212512 (2006).

¹⁶J. S. Daniels, E. P. Anderson, N. Pourmand, and T. H. Lee, presented at the Instrumentation and Measurement Technology Conference (I2MTC), 2010 IEEE, (unpublished).

¹⁷A. M. Rauwerdink and J. B. Weaver, *Appl. Phys. Lett.* **96**, 033702 (2010).